Four-photon Kapitza-Dirac effect as an electron spin filter

Asma Ebadati,[1] Mohsen Vafaee,[2] and Babak Shokri[1,3,*]

[1]*Laser-Plasma Research Institute, Shahid Beheshti University, G. C., Evin, Tehran, Islamic Republic of Iran*

[2]*Department of Chemistry, Tarbiat Modares University, P. O. Box 14115-175, Tehran, Islamic Republic of Iran*

[3]*Physics Department, Shahid Beheshti University, G. C., Evin, Tehran, Islamic Republic of Iran*

(Received 14 March 2018; published 17 September 2018)

We theoretically demonstrate the feasibility of producing an electron spin beam splitter using Kapitza-Dirac diffraction on bichromatic standing waves which are created by the fundamental frequency and its third harmonic. The relativistic electron in the Bragg regime absorbs three photons with a frequency of ω and emits a photon with a frequency of 3ω; we introduce this as the four-photon Kapitza-Dirac effect. In this four-photon Kapitza-Dirac effect distinct spin effects arise in different polarizations of the third harmonic laser beam. It is shown that the shape of the Rabi oscillation between the initial and scattered states is changed and finds two unequal peaks for all polarizations of laser beams. For the case of circular polarization of the fundamental and third harmonic, despite Rabi oscillation, the spin down electron beam in 0.23 fs intervals maintains its momentum and spin. Also we find that if a suitable combination of a linearly polarized fundamental laser beam and a third harmonic with circular polarization in the condition $\vec{p}\cdot\vec{A}$ term is involved, it results in a spin-dependent oscillation that preserves the spin state of the initial electron.

DOI: 10.1103/PhysRevA.98.032505

I. INTRODUCTION

The Stern-Gerlach experiment provided evidence for the existence of spin as an intrinsic, nonclassical property [1]. A beam of silver atoms traveling through an inhomogeneous magnetic field is deflected up or down depending on their spin. Strangely, this experiment did not work with beams of electrons [2]. Bohr and Pauli emphasized that free electrons cannot be spin polarized by exploiting magnetic fields, because of the combined effects of the Lorentz force and quantum uncertainty principle. This conclusion was due to the concept of classical particle trajectories and became a general argument in scientific literature [3–5].

One of the first efforts refuting the Bohr and Pauli statement was using a longitudinal magnetic field configuration instead of the standard transverse geometry of Stern-Gerlach. In this way, the complete spin splitting with quantum-mechanical analysis was reported [6-9]. In recent theoretical studies, the use of the grating and electromagnetic fields resulted in the spin separation for electrons. Tang *et al.* proposed a spin-polarized Talbot effect which is nonparaxial for an electron beam scattered from a grating of magnetic nanostructures [10]. Also a transverse Stern-Gerlach magnet which diffracts electrons by a magnetic phase grating was discussed by McGregor *et al.* [11]. They indicated that by flowing a current to the solenoids, a spin-dependent phase difference is created between the two arms of the Mach-Zehnder interferometer [12]. Moreover, a space-variant Wien filter, named the "q filter," which is composed of space-variant orthogonal electric and magnetic fields can act as an efficient spin-polarization filter. This filter couples spin angular momentum to orbital angular momentum for electron, neutron, or atom beams [13,14].

The Kapitza-Dirac (KD) effect, the quantum-mechanical diffraction of an electron on a periodic spatial structure formed by a standing light wave, confirmed that it could be a way to detect the spin of electrons [15]. Ahrens *et al.* theoretically showed complete spin-flip transitions applying relativistic treatment of the KD effect [16,17]. It was demonstrated that electrons according to their spin state in the interaction with circularly polarized counterpropagating monochromatic standing waves can be separated [18]. In the meantime, Dellweg *et al.* reported a spin-dependent Kapitza-Dirac scattering by using bichromatic ($\omega : 2\omega$) laser beams [19,20]. Also Dellweg showed that spin dynamics of electrons in the bichromatic KD effect is dependent on the polarization of laser beams and therefore the spin direction of the output beams can be controlled [21,22].

One major result of these studies is that the initial electron with spin up state is transferred to the scattered electron with spin down and vice versa. This is symmetric flipping spin dynamics. For two special cases, circularly polarization in the KD effect with equal frequency [18] and combination of linear-circular polarization in the bichromatic KD effect with a frequency ratio of 2 [22], the spin of the electron does not flip and preserves its state.

In the present paper, we theoretically discuss the bichromatic KD effect arising from the interaction of the laser beam with frequency ω and the counterpropagating laser beam with frequency 3ω. In these fields, the electron exchanges four photons and the four-photon bichromatic KD occurs. Recently Kozák discussed the four-photon inelastic scattering and derived the classical stationary ponderomotive potential in an optical standing wave formed by two light waves with frequencies of ω and 3ω [23]. We investigate the spin polar-

*b.shokri@sbu.ac.ir

ization of the electron using various polarized counterpropagating laser beams with a frequency ratio of three. We focus on the electron whose momentum is parallel to the laser beam axis so that the interaction term $\vec{p}\cdot\vec{A}$ becomes insignificant. Our article is organized as follows: In Sec. II we determine that in bichromatic standing waves with a frequency ratio of $1:3$, an electron exchanges four photons. Then based on the S-matrix approach, the transition amplitude for the resonant state is calculated and the polarization-dependent Rabi frequency is taken into account. Numerical solutions of the time-dependent Dirac equation in momentum space are applied to clear up relativistic quantum dynamics in Sec. III and look into the scattering probability result of the different polarizations of two-color beams. In this paper we consider $\hbar = 1$.

II. THEORETICAL DESCRIPTION

A. Electron dispersion in the Bragg regime

The interaction between an electron and two counterpropagating laser fields of frequency ω_i $(i = 1, 2)$ is due to the absorption of some photons from laser beam 1 and the stimulated emission of some photons to laser beam 2. In the case of an intense bichromatic standing wave, the multiphoton interaction between electron and laser field becomes more likely. The absorption of N_a photons with ω_1 frequency and emission of N_e photons with ω_2 frequency conserve energy and momentum if $N_a\omega_1 = N_e\omega_2$. In the case of $\omega_1 = \omega$ and $\omega_2 = 3\omega$, a free electron absorbs three ω photons and emits one 3ω photon or vice versa. Since a photon has the energy $c\hbar k$ and the momentum $\hbar k$, the total transferred energy is $\Delta E = c(N_a k_1 - N_e k_2)$ and the total transferred momentum is $\Delta p = (N_a k_1 + N_e k_2)$. In the presence of the fundamental frequency and its third harmonic with $N_a = 3$ and $N_e = 1$, after the interaction the electron momentum change is $6k$.

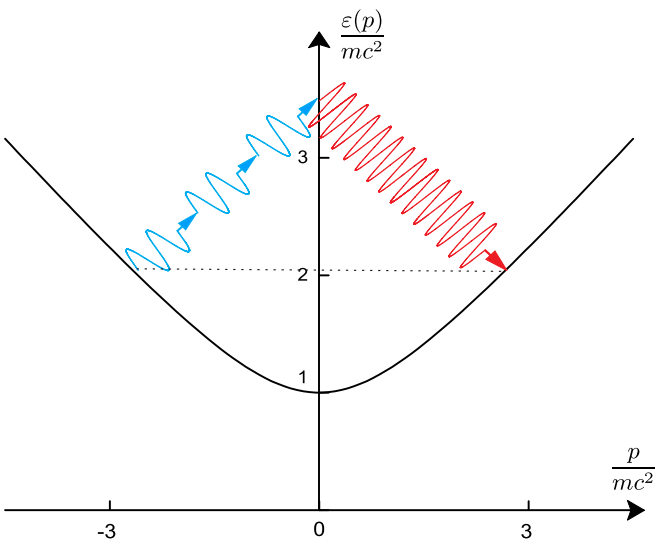

FIG. 1. Sketch of dominant pathway of four-photon KD effect in bichromatic standing waves. The dispersion relation of energy and momentum is in the Bragg regime and each wiggly arrow shows a photon.

The relativistic energy-momentum relation secant and quantum pathway that increases electron momentum by $6k$ are shown in Fig. 1. The total exchange of energy and momentum of the electron with laser beams is represented by the horizontal dashed line. This slope is given by $s = \frac{\Delta E}{\Delta p}$ and connects initial and final momenta of the diffracted electron [17]. All pathways in the Bragg regime start and end exactly on the dispersion relation secant. Theoretically, other transitions are also possible as well, but we focus on the resonant two-state quantum dynamics in the Bragg regime. Absorption of one photon of 3ω and emission of three photons of ω make no difference in the result.

B. S-matrix approach

The evaluation of the relativistic electron in the four-photon Kapitza-Dirac process and in the presence of a given external electromagnetic 4-potential $A = (\phi, \vec{A})$ is described quantum mechanically by the Dirac equation

$$\left[i\not{\partial} + \frac{e}{c}\not{A}(x) - mc\right]\psi(x) = 0, \tag{1}$$

in which $\not{A}$ is denoted by the Feynman slash $\not{A} = \gamma\cdot A$ and γ stands for Dirac matrices.

An analytical treatment for multiphoton-stimulated Compton scattering such as bichromatic Kapitza-Dirac scattering was accomplished through the S-matrix approach with suitable approximations [22]. The Dirac equation has a well-known solution, the Volkov state for an electron in the case of the external potential being a plane wave. By using the fundamental laser mode and Volkov states for the incident electron, the remaining four-photon Kapitza-Dirac process can be represented within first-order perturbation theory [24,25]. We begin with the S matrix as used for multiphoton Compton scattering,

$$S = \frac{ie}{c}\int d^4x\, \bar{\psi}_{p',s'}\not{A}_2\psi_{p,s}. \tag{2}$$

Here $\psi_{p,s}(x)$ is the Dirac-Volkov state with Λ_p a field-dependent term in the exponent:

$$\psi_{p,s}(x) = \sqrt{\frac{mc}{Vp^0}}\left(1 - \frac{e\not{k}_1\not{A}_1(k_1\cdot x)}{2ck_1\cdot p}\right)u_{p,s}e^{-ip\cdot x + i\Lambda_p}, \tag{3}$$

$$\Lambda_p = \frac{1}{ck_1\cdot p}\int^{k_1\cdot x}\left[ep\cdot\mathcal{A}_1(\phi) + \frac{e^2}{2c}\mathcal{A}_1^2(\phi)\right]d\phi. \tag{4}$$

The calculation of the S matrix is the same as that used in the three-photon KD effect, except that a further photon participates in the interaction [22]. In the case of a vector potential as a plane wave regarding radiation gauge $A_1(k_1\cdot x) = A_1(x)$, and with a complex polarization 4-vector $\epsilon_1 = (0, \vec{\epsilon})$, and the wave 4-vector $k_1 = \frac{\omega}{c}(1, \vec{e}_z)$, satisfying $\epsilon_1^*\cdot\epsilon_1 = -1$ and $\epsilon_1\cdot k_1 = 0$. A similar notation is employed for the counterpropagating wave $A_2(x)$ with ϵ_2 and $k_2 = 3k_1 = 3k$, respectively. In the presence of the third harmonic the S matrix for transition from p to p' by absorbing three photons from A_1 as a beam with fundamental frequency and emitting one photon into A_2 as a beam with 3ω frequency is

given by

$$S \approx \frac{ie}{\hbar c V}\int d^4x\,\bar{u}_{p',s'}\Bigg(\not{A}_2^{(+)}\tilde{J}_3 e^{i(p'-p-3k_1)\cdot x} - \frac{e}{2c}\left[\frac{\not{A}_1^{(-)}\not{k}_1\not{A}_2^{(+)}}{k_1\cdot p'} + \frac{\not{A}_2^{(+)}\not{k}_1\not{A}_1^{(-)}}{k_1\cdot p}\right]\tilde{J}_2 e^{i(p'-p-2k_1)\cdot x} + \frac{e^2}{4c^2}\left[\frac{\not{A}_1^{(-)}\not{k}_1\not{A}_2^{(+)}\not{k}_1\not{A}_1^{(-)}}{(k_1\cdot p')(k_1\cdot p)}\right]\tilde{J}_1 e^{i(p'-p-k_1)\cdot x}\Bigg)u_{p,s}$$
$$\approx \frac{ie}{2\hbar}T\bar{u}_{p',s'}\left[a_2\tilde{J}_3\bar{\not{\epsilon}}_2 - \frac{ea_1a_2}{4c}\tilde{J}_2\left(\frac{\not{\epsilon}_1\not{k}_1\bar{\not{\epsilon}}_2}{k_1\cdot p'} + \frac{\bar{\not{\epsilon}}_2\not{k}_1\not{\epsilon}_1}{k_1\cdot p}\right) + \frac{e^2a_1^2a_2}{16c^2}\tilde{J}_1\frac{\not{\epsilon}_1\not{k}_1\bar{\not{\epsilon}}_2\not{k}_1\not{\epsilon}_1}{(k_1\cdot p')(k_1\cdot p)}\right]u_{p,s}. \quad (5)$$

Here, $\not{A}_1^{(-)} = \frac{1}{2}a_1\not{\epsilon}_1 e^{-ik_1\cdot x}$ is the component that defines the absorption of one photon from A_1 with $\not{\epsilon}_1 = \epsilon_1\cdot\gamma$, and $\not{A}_2^{(+)} = \frac{1}{2}a_2\bar{\not{\epsilon}}_2 e^{ik_2\cdot x}$, where $\bar{\not{\epsilon}}_2 = \epsilon_2^*\cdot\gamma$ is the component that describes emission of one photon into A_2. Also $\tilde{J}_{1,2,3}$ are generalized Bessel functions. In this derivation only the resonant scattering process was considered, which fulfills the Bragg condition. Therefore the d^4x integration does result in the factor cVT, with T the interaction time and V quantification volume [22]. The initial and scattered electron momenta are set respectively to $p = (p^0, p_x, 0, -3\hbar k)$ and $p' = (p^0, p_x, 0, +3\hbar k)$. The Dirac spinors for theses momenta are corresponding to Pauli spinors by

$$u_{(p,s)} = \frac{1}{\sqrt{2mc(p^0+mc)}}\begin{pmatrix}(p^0+mc)\chi_s\\ \vec{p}\cdot\vec{\sigma}\,\chi_s\end{pmatrix}. \quad (6)$$

We can calculate a part of Eq. (5) as

$$(\bar{u}_{p',s'}\bar{\not{\epsilon}}_2 u_{p,s})_{s',s} = -\frac{p_x}{mc}\vec{\epsilon}_2^{\,*}\cdot\vec{e}_x + \frac{3i\hbar\omega}{mc^2}(\vec{\epsilon}_2^{\,*}\times\vec{e}_z)\cdot\vec{\sigma} \quad (7)$$

and in a similar way for the second part

$$\left(\bar{u}_{p',s'}\left[\frac{\not{\epsilon}_1\not{k}_1\bar{\not{\epsilon}}_2}{k_1\cdot p'} + \frac{\bar{\not{\epsilon}}_2\not{k}_1\not{\epsilon}_1}{k_1\cdot p}\right]u_{p,s}\right)_{s',s} \approx \frac{2\vec{\epsilon}_1\cdot\vec{\epsilon}_2^{\,*}}{mc} - \frac{6i\hbar\omega}{m^2c^3}(\vec{\epsilon}_1\times\vec{\epsilon}_2^{\,*})\cdot\vec{\sigma}. \quad (8)$$

The other term of the S matrix in Eq. (5) due to $(k\cdot\sigma)^2 = 0$ is zero. Also from the Taylor series of the generalized Bessel functions, we can estimate

$$\tilde{J}_1 \approx -3\frac{ea_1}{mc^2}\frac{p_x}{mc}\vec{\epsilon}_1\cdot\vec{e}_x,$$
$$\tilde{J}_2 \approx \frac{e^2a_1^2}{m^2c^4}\left(\frac{9}{2}\frac{p_x^2}{m^2c^2}(\vec{\epsilon}_1\cdot\vec{e}_x)^2 - \frac{3}{8}\vec{\epsilon}_1^{\,2}\right),$$
$$\tilde{J}_3 \approx \frac{e^3a_1^3}{m^3c^6}\left(-\frac{9}{2}\frac{p_x^3}{m^3c^3}(\vec{\epsilon}_1\cdot\vec{e}_x)^3 + \frac{9}{8}\frac{p_x}{mc}(\vec{\epsilon}_1\cdot\vec{e}_x)\vec{\epsilon}_1^{\,2}\right). \quad (9)$$

Putting all this together, the S matrix of Eq. (5) for small transverse momentum is estimated as follows:

$$S \approx \frac{i}{2}T\frac{e^4a_1^3a_2}{m^4c^8}\left[\frac{27i}{8}\frac{p_x}{mc}\omega(\vec{\epsilon}_1\cdot\vec{e}_x)\vec{\epsilon}_1^{\,2}(\vec{\epsilon}_2^{\,*}\times\vec{e}_z)\cdot\vec{\sigma} - \frac{9i}{16}\omega\vec{\epsilon}_1^{\,2}(\vec{\epsilon}_1\times\vec{\epsilon}_2^{\,*})\cdot\vec{\sigma} - \frac{9}{4\hbar}\frac{p_x^2}{m}(\vec{\epsilon}_1\cdot\vec{\epsilon}_2^{\,*})(\vec{\epsilon}_1\cdot\vec{e}_x)^2 - \frac{9}{8\hbar}\frac{p_x^2}{m}(\vec{\epsilon}_1\cdot\vec{e}_x)\vec{\epsilon}_1^{\,2}(\vec{\epsilon}_2^{\,*}\cdot\vec{e}_x)\right] = \frac{i}{2}T\xi_1^3\xi_2\hat{\Omega}. \quad (10)$$

For order in m^{-1}, we derive the Rabi frequency as

$$\hat{\Omega} = -\frac{9i}{16}\omega\vec{\epsilon}_1^{\,2}(\vec{\epsilon}_1\times\vec{\epsilon}_2^{\,*})\cdot\vec{\sigma} + \frac{27i}{8}\frac{p_x}{c}\omega(\vec{\epsilon}_1\cdot\vec{e}_x)\vec{\epsilon}_1^{\,2}(\vec{\epsilon}_2^{\,*}\times\vec{e}_z)\cdot\vec{\sigma}. \quad (11)$$

Here, $\xi_{1,2} = \frac{ea_{1,2}}{mc^2}$ are the common dimensionless field amplitudes used in atomic physics. It is worth noting that the terms with $\frac{p_x^2}{\hbar}$ in Eq. (10) are of the same order as the $\frac{p_x\omega}{c}$ term, but the latter is the more effective term for electron spin dynamics. The Rabi frequency is indicated for various combinations of polarizations of laser beams in Table I.

TABLE I. The Rabi frequency $\hat{\Omega}$ for various polarizations of bichromatic ($\omega : 3\omega$) standing waves. The definition $\sigma_\pm = \sigma_x \pm i\sigma_y$ is applied.

Case	$\vec{\epsilon}_1$	$\vec{\epsilon}_2$	$\hat{\Omega}_{\omega:3\omega}$
1	$\vec{e}_x$	$\vec{e}_x$	$-\frac{27i}{8}\frac{p_x\omega}{c}\sigma_y$
2	$\vec{e}_x$	$\vec{e}_y$	$\frac{27i}{8}\frac{p_x\omega}{c}\sigma_x - \frac{9i}{16}\omega\sigma_z$
3	$\frac{1}{\sqrt{2}}(\vec{e}_x + i\vec{e}_y)$	$\frac{1}{\sqrt{2}}(\vec{e}_x + i\vec{e}_y)$	0
4	$\frac{1}{\sqrt{2}}(\vec{e}_x - i\vec{e}_y)$	$\frac{1}{\sqrt{2}}(\vec{e}_x - i\vec{e}_y)$	$\frac{-27}{16}\frac{p_x\omega}{c}\sigma_+ + \frac{9}{16}\omega\sigma_z$
5	$\frac{1}{\sqrt{2}}(\vec{e}_x + i\vec{e}_y)$	$\vec{e}_x$	0
6	$\frac{1}{\sqrt{2}}(\vec{e}_x - i\vec{e}_y)$	$\vec{e}_x$	$\frac{-27i}{8\sqrt{2}}\frac{p_x\omega}{c}\sigma_y + \frac{9}{16\sqrt{2}}\omega\sigma_z$
7	$\vec{e}_x$	$\frac{1}{\sqrt{2}}(\vec{e}_x + i\vec{e}_y)$	$\frac{27}{8\sqrt{2}}\frac{p_x\omega}{c}\sigma_- - \frac{9}{16\sqrt{2}}\omega\sigma_z$
8	$\vec{e}_x$	$\frac{1}{\sqrt{2}}(\vec{e}_x - i\vec{e}_y)$	$\frac{-27}{8\sqrt{2}}\frac{p_x\omega}{c}\sigma_+ + \frac{9}{16\sqrt{2}}\omega\sigma_z$

III. NUMERICAL RESULTS

In this section, the numerical results will be presented for the spin-dependent Kapitza-Dirac scattering in bichromatic counterpropagating laser fields with a frequency ratio of 3. Taking into account the combined vector potential and rewriting the Dirac equation in momentum space, we find a system of coupled ordinary differential equations. The numerical solution of differential equations is obtained by employing a Crank-Nicholson scheme [17]. The solutions are the absolute square values of the expansion coefficients that represent scattering probability of the electron in the particular quantum state. $c_n^\zeta(n = 0, \pm1, \pm2, \ldots)$ coefficients represent electrons with momentum $p_n = (p_x, 0, nk)$. The index $\zeta \in \{+\uparrow, +\downarrow, -\uparrow, -\downarrow\}$ labels the sign of the energy and the spin direction. These states can be denoted by $|nk, \zeta\rangle$.

In the four-photon KD effect, the vector potential for the bichromatic field ($\omega : 3\omega$) can be described in the form of

$$\vec{A} = A_1\{\cos[k(z \pm ct)]\hat{\epsilon}_1\} + A_2\{\cos[3k(z \pm ct)]\hat{\epsilon}_2\}, \quad (12)$$

where A_1 and A_2 are the amplitudes of standing waves and ϵ_1, ϵ_2 are polarization vectors. The electron with initial longitudinal momentum of $p_z = -3k$ in presence of the mentioned vector potential is scattered into mirror mode with longitudinal momentum $p_z = +3k$ by exchanging $6k$ momentum. For all the next calculations, we start with longitudinal momentum $p_z = -3k$ and spin projection either up or down, while the other momentum modes at initial time will be zero. As mentioned in the Bragg regime, transfer of population is restricted to $p_z = +3k$ for the final state and the occupation probability of other momentum modes is very small. When the electron has a component perpendicular to the laser beam direction, all four states $|-3, +\uparrow\rangle$, $|-3, +\downarrow\rangle$, $|+3, +\uparrow\rangle$, and $|+3, +\downarrow\rangle$ participate in the interaction. It is worth noting that because of focusing on the effect of $\vec{\sigma}\cdot\vec{B}$ in this work, we choose the electron momentum to be parallel to the axis of the laser beam; however practically the influence of $\vec{p}\cdot\vec{A}$ cannot be ignored.

In all simulations, smooth switchings on and off laser fields are $\sin^2$ slopes for five-cycle laser periods with a flat-top function. To study spin effects in four-photon KD diffraction, the following various polarizations of this bichromatic standing wave are considered.

A. Linear polarization for two laser beams (lin-lin)

In the first setup, the fundamental field and its third harmonic are linearly polarized along the x axis:

$$\vec{A} = A_1\{\cos[k(z-ct)]\hat{e}_x\} + A_2\{\cos[3k(z+ct)]\hat{e}_y\}. \quad (13)$$

The incident electron is $-3\hbar k$ along the laser propagation direction and has no component parallel to the polarization direction. The overall laser intensity in the lin-lin setup is $I = \frac{\omega^2 A_1^2 + (3\omega)^2 A_2^2}{8\pi c}$, when the amplitudes of beams are at maximum of their values. The laser parameters of the fundamental laser beam for all numerical solutions correspond to a peak intensity of 2×10^{22} W cm^{-2} and a photon energy of 2.0 keV. The corresponding laser parameter can be attained from high-power x-ray free-electron lasers such as the European XEFEL (Hamburg) or LCLS (Stanford) [26]. Figure 2 presents the typical behavior of an electron in both linear laser beams. For the electron that is injected with spin up, a Rabi oscillation takes place between $|-3, +\uparrow\rangle$ and $|+3, +\downarrow\rangle$. The interaction in this field configuration is independent of the initial electron spin state so that the electron at initial momentum and the spin down state $|-3, +\downarrow\rangle$ is also scattered into the reflected momentum and spin up state $|+3, +\uparrow\rangle$ and the Rabi oscillation is similarly as in Fig. 2. This symmetry of spin flipping exists also in the three-photon bichromatic ($\omega:2\omega$) KD effect with linear polarization [22].

The shape of oscillation in the bichromatic four-photon KD effect is sinusoidal and has two distinct peaks that are different in size in Fig. 2. The probability of $|c_{-3}^{+\uparrow}|^2$ has a sinusoidal oscillation whose minimum amplitude alternatively changes between 0.22 and 0.0 while $|c_{+3}^{+\downarrow}|^2$ oscillates similarly to $|c_{-3}^{+\uparrow}|^2$ but its maximum amplitude changes between 0.78 and 1.0. The Rabi oscillation period is about 2.8 fs and simulation shows that even with changing the standing-wave amplitudes,

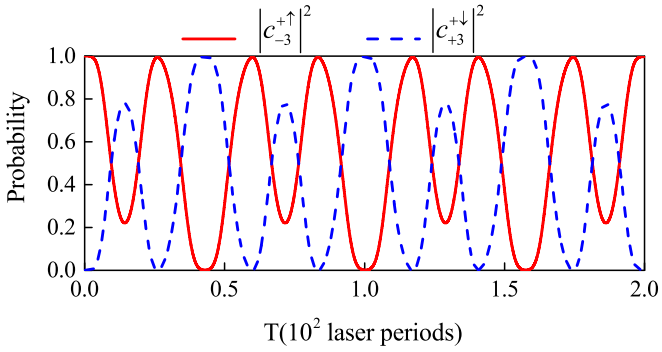

FIG. 2. Temporal evolution of the occupation probability in four-photon KD effect with linear fundamental beam and counterpropagating linear third harmonic. The overall laser intensity is 8.8×10^{22} W cm^{-2} with wavelength $\lambda = 0.6$ nm; field parameters for beam ω and 3ω are $eA_1 = 6\times10^4$ eV and $eA_2 = 2\times10^4$ eV, respectively. The electron enters the laser fields with $p_z = -3k$ along the laser field direction.

these two distinct peaks for $|c_{-3}^{+\uparrow}|^2$ and $|c_{+3}^{+\downarrow}|^2$ will not be destroyed.

The vector potential $A(x) = f(t)[A_1(k_1\cdot x) + A_2(k_2\cdot x)]$ with slow envelope function $f(t)$ in the bichromatic ($\omega:2\omega$) KD effect results in a typical Rabi oscillation with one peak [22]. Our results confirm that with similar vector potential for the bichromatic ($\omega:3\omega$) KD effect

$$\vec{A} = f(t)\{A_1[\cos(kz)\hat{e}_x] + A_2[\cos(3kz)\hat{e}_x]\}, \quad (14)$$

the typical oscillatory behavior with sinusoidal oscillation appears as shown in Fig. 3. The Rabi cycle is fully developed in Fig. 3 and the period of Rabi oscillation is $2\pi/\Omega_R = 0.84$ fs. By comparing vector potentials mentioned in Eq. (13) and Eq. (14), it is obvious that the existence of the $\cos(\omega_{i=1,2}t)$ part of numerical solutions results in different oscillation behavior.

B. Corotating circular fundamental and third harmonic fields (cir-cir)

We now look over an electron in two circular bichromatic counterpropagating but corotating waves

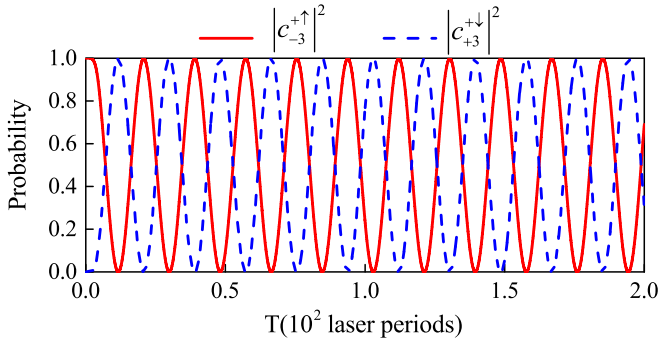

FIG. 3. Rabi oscillation in both linear polarization setups for vector potential mentioned in Eq. (13). All other laser and electron parameters are the same as in Fig. 2.

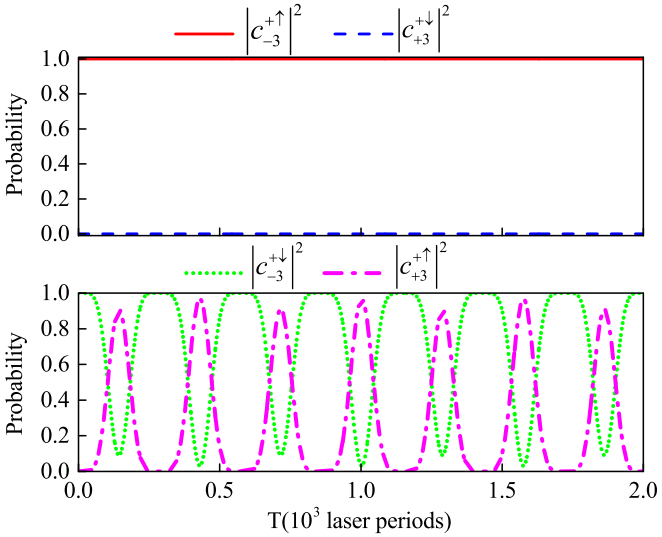

FIG. 4. Temporal evolution of the occupation probability in four-photon KD effect with corotating circular bichromatic waves. The combined laser intensity is 19×10^{23} W cm^{-2} with wavelength $\lambda = 0.6$ nm; field amplitude for both beams is $eA_1 = eA_2 = 9 \times 10^4$ eV. The electron enters the laser fields with $p_z = -3k$ along the laser direction. Upper panel of the figure shows that an electron with spin up does not scatter in this setup.

given by

$$\vec{A} = \frac{A_1}{\sqrt{2}}[\cos(kz)\cos(ckt) + \cos(3kz)\cos(3ckt)](\hat{e}_x) - \frac{A_2}{\sqrt{2}}[\sin(kz)\cos(ckt) - \sin(3kz)\cos(3ckt)](\hat{e}_y). \tag{15}$$

If the electron is initially in $|-3, +\uparrow\rangle$, no diffraction occurs at all as shown in the upper panel of Fig. 4. In contrast, for the electron with spin down and initial momentum $-3k$ in the lower panel, a Rabi oscillation between two states $|-3, +\downarrow\rangle$ and $|+3, +\uparrow\rangle$ takes place in this configuration. This spin-dependent diffraction behavior implies that it is possible to separate electrons based on their initial spin state in circularly polarized laser beams. The effective scattering term of the Rabi matrix is expected to be proportional to σ_+ due to the spin-dependent behavior, but the result of Table I in this configuration, for an electron with momentum parallel to the laser propagation, shows only the σ_z term. Considering the high nonlinear scattering, only our numerical simulations confirm that the electron with spin up and momentum $-3k$ is not diffracted. It is interesting to say that the electron with initial $|-3, +\uparrow\rangle$ state in these fields polarization can be diffracted, provided that it has a momentum in the x direction. We find from numerical results that the electron with initial $|-3, +\uparrow\rangle$ state maintains its spin state and oscillates between $|-3, +\uparrow\rangle$ and $|+3, +\uparrow\rangle$ modes.

The shape of Rabi oscillation in the cir-cir setup for an electron with spin down is interesting too. Two distinguished peaks in oscillation exist. The maximum values of peaks are 0.90 and 0.96; the difference in maximum of these peaks is less in this setup. As represented in Fig. 4, for an interval of about 0.23 fs the population of modes does not transfer and the electron maintains its momentum and spin. In fact, similarly to Fig. 2 the electron does not have instant varying momentum and spin and the modes with time delay exchange their population. Also in this setup, the vector potential without the $\cos(ck_i t)$ and $\cos(3ck_i t)$ parts in Eq. (15) results in a typical sinusoidal Rabi oscillation similar to Fig. 3.

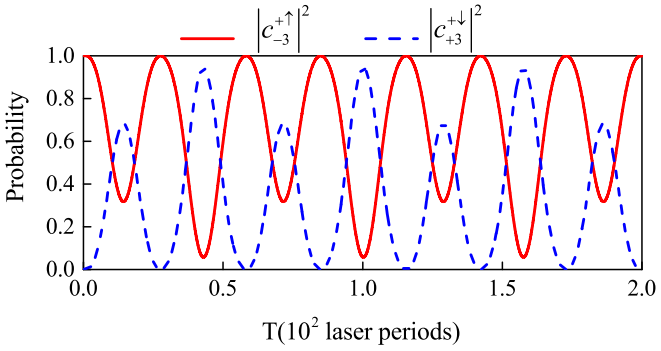

FIG. 5. Temporal evolution of the occupation probability in four-photon KD effect with a hybrid setup that the fundamental laser beam is linear and the third harmonic is circularly polarized. The other simulation parameters are the same as in Fig. 2. The electron just has momentum $-3k$ along the laser propagation.

C. Combination of linear and circular polarization fields (lin-cir)

To examine the result of the last section about spin separation, we focus on a bichromatic setup in which the fundamental beam is linearly polarized and the third harmonic beam is circularly polarized:

$$\vec{A} = \left[\cos(kz)\cos(ckt) + \frac{A_2}{\sqrt{2}}\cos(3kz)\cos(3ckt)\right](\hat{e}_x) - \frac{A_2}{\sqrt{2}}[\sin(3kz)\cos(3ckt)](\hat{e}_y). \tag{16}$$

When the electron has no momentum along the field's polarization direction ($p_x = p_y = 0$), by choosing the high-frequency beam to be circularly polarized, the Rabi oscillation for spin up and spin down electrons at $-3\hbar k$ momentum occurs. As shown in Fig. 5, a similar oscillation with spin-flipping symmetry happens for both spin states of the electron. The Rabi period is 2.8 fs and with the same field amplitudes as the lin-lin setup, the population of modes does not transfer completely. The maximum of Rabi amplitude of the $|+3, +\downarrow\rangle$ state only reaches 0.94. According to case 7 of Table I, the Rabi matrix in this setup with $p_x = 0$ is proportional to $\hat{\Omega} = \frac{-9}{16\sqrt{2}}\omega\sigma_z$. Therefore the analytical frequency has no spin-dependent term contribution and the numerical result in Fig. 5 confirms that. In this setup, the Rabi oscillation with the symmetry of spin flipping exists for the electron without influence of $\vec{p} \cdot \vec{A}$.

By choosing $p_x = 2\hbar k$ in the hybrid polarization setup where the low-frequency beam is linearly polarized and the third harmonic beam is circularly polarized, all four allowed states $|-3, +\uparrow\rangle$, $|-3, +\downarrow\rangle$, $|+3, +\uparrow\rangle$, and $|+3, +\downarrow\rangle$ make

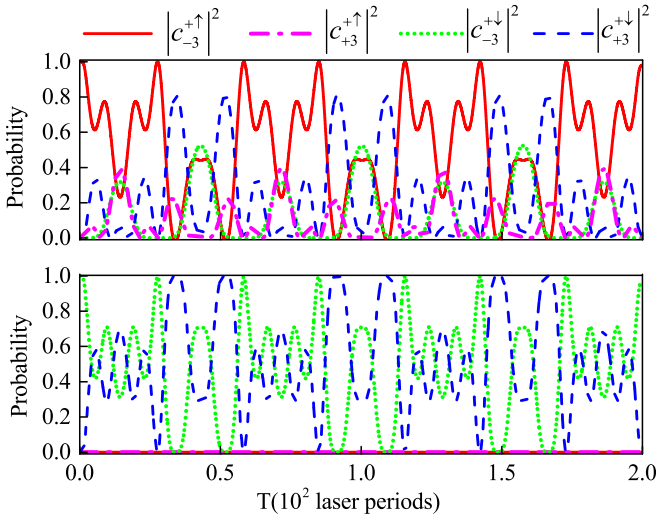

FIG. 6. Temporal evolution of the occupation probability in four-photon KD effect from a linear polarized fundamental laser beam and third harmonic with circularly polarization. The fundamental laser wavelength $\lambda = 0.6$ nm and field amplitudes are the same as in Fig. 2. The incident electron spin up with $p_x = 2\hbar k$, in upper panel, after interaction is diffracted to $+3k$ momentum and maintains its spin state. For spin down electron, in lower panel, the four allowed modes are populated.

very complicated oscillations. Figure 6 indicates numerical simulation for spin up and down electron behavior in these circumstance. In the upper panel when the initial electron spin is pointing upwards, all four modes populated. When the electron spin is down and has $-3k$ momentum, the simulation starting from $|-3,+\downarrow\rangle$ only travels to the $|+3,+\downarrow\rangle$ state and there is no spin-flipping oscillation. A clear spin-dependent Rabi oscillation emerges in this setup for either right or left handed circular polarization of the third harmonic laser beam, which also was predicted by the S-matrix method (cases 7 and 8 in Table I). The existence of $\sigma_{\mp}$ in Rabi frequency cause a spin-preserving transition for the spin down and spin up electrons, respectively.

For the case with a fundamental frequency beam of circular polarization and a third harmonic beam of linear polarization and electron with $p_x = 0$, the spin-flipping symmetry still exists; i.e., by choosing $c_{-3}^{+\uparrow}(t=0) = 1$ or $c_{-3}^{+\downarrow}(t=0) = 1$, the population is transferred to $|+3,+\downarrow\rangle$ and $|+3,+\uparrow\rangle$, respectively. We have a Rabi oscillation similar to Fig. 5 for both electron spin states. Furthermore for the electron with p_x, the Rabi frequency $\hat{\Omega} = \frac{-27i}{8\sqrt{2}}\frac{p_x\omega}{c}\sigma_y + \frac{9}{16\sqrt{2}}\omega\sigma_z$ derived in Table I predicts that there is an oscillation for any state of spin electron. This means that the electron with or without p_x oscillates with spin-flipping symmetry. Our numerical results show Rabi oscillation for this setup, whether the electron has a momentum along laser polarization or not.

IV. CONCLUSION

Four-photon Kapitza-Dirac scattering occurs in the bichromatic standing wave when the electron beam absorbs three photons from the laser field with ω frequency and emits one photon to the counterpropagation laser beam with 3ω frequency. The initial electron spin and photon helicity are two factors that can affect the polarization of the free electron in the four-photon bichromatic $(\omega : 3\omega)$ KD effect. In this work, it is shown that when the fundamental and third harmonic laser beams are linearly and circularly polarized, respectively, Rabi oscillation occurs for spin up and down electrons that only have momentum along laser propagation. But when the initial electrons have a momentum component parallel to laser polarization, the symmetric spin-flipping effect disappears.

In this study, we showed that the shape of the Rabi frequency in the bichromatic $(\omega : 3\omega)$ vector potential has two unequal peaks that change with beam amplitude and the laser intensity. This different shape of oscillation is due to the fast time varying $\cos(ck_i t)$ part of the vector potential. Our results also indicate that these two distinct peaks in the Rabi oscillation exist for other harmonics such as second and fourth harmonics.

Four-photon KD numerical simulation in this work shows that spin-flip transitions happen in lin-lin and lin-cir setups for zero p_x, except for the corotating circular laser beams in which the electron with spin up remains in its initial spin state. For the combination of the linear fundamental and circular third harmonic beams, when the $\vec{p}\cdot\vec{A}$ term is involved for $p_x \neq 0$, the spin preserving occurs for the spin up/down electron beam. This situation also was predicted by the Pauli theory for circularly polarized fields [18,27].

In summary, the corotating circular configuration in the bichromatic $(\omega : 3\omega)$ standing wave acts as a spin polarizer. It was shown that by choosing properly linear and circular polarizations for low and high frequencies of laser beams and nonzero p_x, the spin-flipping transition is stopped for electrons and the electrons maintain their initial spin state.

[1] W. Gerlach and O. Stern, Z. Phys. **9**, 353 (1922).
[2] N. F. Mott and S. H. W. Massey, *The Theory of Atomic Collisions* (Clarendon, Oxford, 1965), pp. 214–219.
[3] W. Pauli, *General Principles of Quantum Mechanics*, translated by P. Achuthan and K. Venkatesan (Berlin, Springer, 1980), Chap. 23, see p. 174.
[4] B. M. Garraway and S. Stenholm, Contemp. Phys. **43**, 147 (2002).
[5] O. Darrigol, Hist. Stud. Phys. Sci. **15**, 39 (1984).
[6] H. Batelaan, T. J. Gay, and J. J. Schwendiman, Phys. Rev. Lett. **79**, 4517 (1997).
[7] G. A. Gallup, H. Batelaan, and T. J. Gay, Phys. Rev. Lett. **86**, 4508 (2001).
[8] G. H. Rutherford and R. Grobe, Phys. Rev. Lett. **81**, 4772 (1998).
[9] G. H. Rutherford and R. Grobe, J. Phys. A **31**, 9331 (1998).
[10] W. X. Tang, D. M. Paganin, and W. Wan, Phys. Rev. B **85**, 064418 (2012).

[11] S. McGregor, R. Bach, and H. Batelaan, New J. Phys. **13**, 065018 (2011).
[12] S. McGregor, W. C.-W. Huang, B. A. Shadwick, and H. Batelaan, Phys. Rev. A **92**, 023834 (2015).
[13] E. Karimi, L. Marrucci, V. Grillo, and E. Santamato, Phys. Rev. Lett. **108**, 044801 (2012).
[14] V. Grillo, L. Marrucci, E. Karimi, R. Zanella, and E. Santamato, New J. Phys. **15**, 093026 (2013).
[15] P. L. Kapitza and P. A. Dirac, Math. Proc. Cambridge Philos. Soc. **29**, 297 (1933).
[16] S. Ahrens, H. Bauke, C. H. Keitel, and C. Muller, Phys. Rev. Lett. **109**, 043601 (2012).
[17] S. Ahrens, H. Bauke, C. H. Keitel, and C. Müller, Phys. Rev. A **88**, 012115 (2013).
[18] S. Ahrens, Phys. Rev. A **96**, 052132 (2017).
[19] M. M. Dellweg and C. Müller, Phys. Rev. A **91**, 062102 (2015).
[20] M. M. Dellweg, H. M. Awwad, and C. Müller, Phys. Rev. A **94**, 022122 (2016).
[21] M. M. Dellweg and C. Müller, Phys. Rev. Lett. **118**, 070403 (2017).
[22] M. M. Dellweg and C. Müller, Phys. Rev. A **95**, 042124 (2017).
[23] M. Kozák, Phys. Rev. A **98**, 013407 (2018).
[24] D. M. Volkov, Z. Phys **94**, 250 (1935).
[25] V. I. Ritus, J. Russ. Laser Res. **6**, 497 (1985).
[26] For current information, see http://www.xfel.eu and https://lcls.slac.stanford.edu.
[27] R. Erhard and H. Bauke, Phys. Rev. A **92**, 042123 (2015).